

Influence of Nonionic Surfactant on the Carbon Steel Corrosion in Hydrochloric Acid Solution

Ahmed A. Farag¹, I. M. Ibrahim²

¹Additives Laboratory, Petroleum Applications Department, Egyptian Petroleum Research Institute (EPRI)
1 Ahmed El-Zomor St., Nasr City, 11727, Cairo, Egypt

²Asphalt Laboratory, Petroleum Applications Department, Egyptian Petroleum Research Institute (EPRI)
1 Ahmed El-Zomor St., Nasr City, 11727, Cairo, Egypt

Abstract: In this study, the inhibition effect of Polyoxyethylene-20-sorbitan monooleate (TW80) on carbon steel corrosion in 1 M HCl solution was studied. For this aim, electrochemical techniques such as potentiodynamic polarization and electrochemical impedance spectroscopy (EIS) were used. Polarization measurements indicated that, the studied inhibitor acts as mixed-type inhibitor. The adsorption of TW80 molecules on the carbon steel surface obeys Langmuir adsorption isotherm. The thermodynamic parameters such as the adsorption equilibrium and the free energy of adsorption are calculated and discussed.

Keywords: Corrosion inhibitor, Nonionic Surfactant, Carbon Steel, Hydrochloric Acid, Adsorption.

1. Introduction

Iron and its alloys could corrode during the acidic applications such as pickling, industrial acid cleaning, acid de-scaling, and also widely applied to enhance oil/gas recovery through acidification in the oil and gas industry, particularly with the use of hydrochloric acid and sulfuric acid, which results in terrible waste of both resources and money [1].

Steel pipelines play an important role in transporting gases and liquids throughout the world. Therefore, the prevention of metals used in petroleum field and industrial applications from corrosion is vital that must be dealt with especially in acid media [2]. The development of corrosion inhibitors is based on organic compounds containing nitrogen, oxygen, sulfur atoms, and multiple bonds in the molecules that facilitate adsorption on the metal surface [3].

The corrosion inhibition efficiency of organic compounds is related to their adsorption properties. Adsorption depends on the nature and the state of the metal surface, on the type of corrosive medium and on the chemical structure of the inhibitor [4]. The choice of inhibitors is based on two considerations:

- First, they could be synthesized conventionally from relatively cheap raw materials;
- Second, they contain the electron clouds on the aromatic rings or, the electronegative atoms such as benzene ring.

Recently, the application of surfactants as effective corrosion inhibitors has attracted the attention of many researchers. The adsorption of the surfactant molecules through their hydrophilic head changes the corrosion resistance property of the metal [5].

In particular nonionic surfactants (where the polar head group is without charge) have been shown to possess high inhibition efficiency for metal corrosion in different solutions. This class of surfactants has substantially lower

critical micelle concentrations (CMCs) than the corresponding ionic surfactants. Generally, the surfactant with lower CMC has the greater tendency to adsorb at the solid surface.

The objectives of this work were to study the inhibition performance of Polyoxyethylene-20-sorbitan monooleate (TW80) (Figure 1) on carbon steel corrosion in 1 M HCl solution using potentiodynamic polarization and electrochemical impedance spectroscopy. Thermodynamic parameters of inhibitor adsorption on the metal surface and metal were also studied.

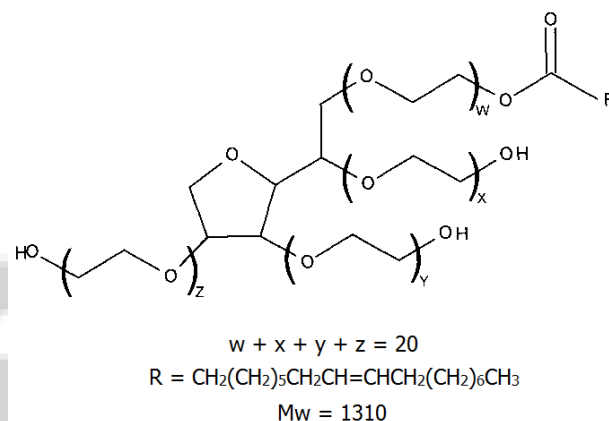


Figure 1: Molecular structures of TW80

2. Experimental

2.1. Material

Tests were performed on carbon steel of the following composition (wt.%): 0.07% C, 0.24% Si, 1.35% Mn, 0.017% P, 0.005% S, 0.16% Cr, 0.18% Ni, 0.12% Mo, 0.01% Cu and the remainder Fe.

2.2. Solutions

The inhibitors solutions with various concentrations were prepared in 1 M HCl. The corrosion tests were performed in HCl solution in the absence and presence of various concentrations of TW80. The aggressive solution of 1 M HCl was prepared by dilution of analytical grade 37% HCl with distilled water. For each experiment, a freshly prepared solution was used under air atmosphere without stirring at 298 K.

2.3. Gravimetric measurements

The carbon steel coupons of 7.0 cm × 2.0 cm × 0.03 cm were abraded with a series of emery paper beginning from 400 to 1200, degreased with acetone, rinsed with distilled water and dried in hot air. After weighing accuracy, the specimens were immersed in 150 ml beaker, which contained 150 ml hydrochloric acid with and without the addition of various concentrations of inhibitor. All the aggressive acid solutions were open to air. After 24 h, the specimens were taken out, washed, dried, and weighed accurately. In order to get good reproducibility, the experiments were carried out in triplicate, and the average weight loss of three parallel carbon steel coupons was reported. The corrosion rate (v) was calculated from the following equation:

$$v = \frac{W}{St} \tag{1}$$

where W is the average weight loss of three parallel carbon steel coupons, S the total area of one steel coupon, and t is immersion time (24 h).

With the calculated corrosion rate, the inhibition efficiency (η_g) of inhibitors on the corrosion of carbon steel was calculated as follows [6]:

$$\eta_g = \frac{v_0 - v}{v_0} \times 100 \tag{2}$$

where v_0 and v are the values of the corrosion rate without and with the addition of the TW80, respectively.

2.4. Electrochemical measurements

The electrochemical measurements were carried out using Volta lab 40 (Tacussel-Radiometer PGZ301) potentiostat and controlled by Tacussel corrosion analysis software model (Voltmaster 4) at under static condition. The corrosion cell used had three electrodes.

The reference electrode was a saturated calomel electrode (SCE). A platinum electrode was used as auxiliary electrode. Carbon steel coupons having the area of 1 cm² were used as a working electrode. The working electrode was immersed in test solutions for 30 minutes to a establish steady state open circuit potential (E_{ocp}). After measuring the E_{ocp} , the electrochemical measurements were performed. The EIS experiments were conducted in the frequency range with high limit of 10⁵ Hz and different low limit 10⁻² Hz at open circuit potential. The polarization curves were obtained in the potential range from -900 to -200 mV(SCE) with 0.5 mV s⁻¹ scan rate.

3. Results and Discussion

3.1. Gravimetric measurements

Table 1 showed the values of corrosion rates (mg cm⁻² h⁻¹), surface coverage (θ) and inhibition efficiencies (η_g) obtained from gravimetric measurements in the absence and presence of various concentrations of TW80 for 24 h immersion in 1 M HCl at 298 K. The variation of corrosion rates (v) with inhibitor concentrations is shown in Figure 2, while the variation of inhibition efficiencies (η_g) with inhibitor concentrations is shown in Figure 3.

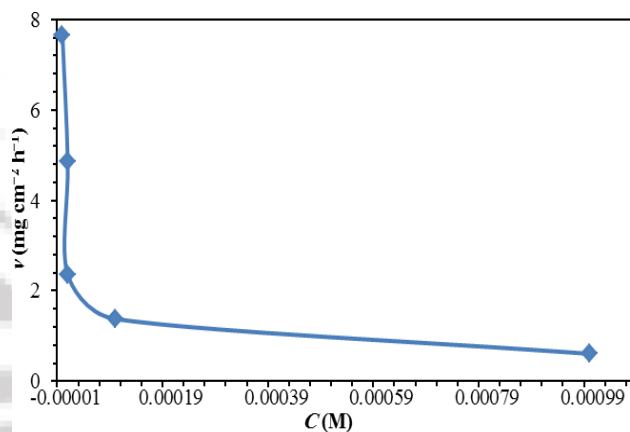


Figure 2: Relationship between the corrosion rate and inhibitor concentration for carbon steel at 298 K

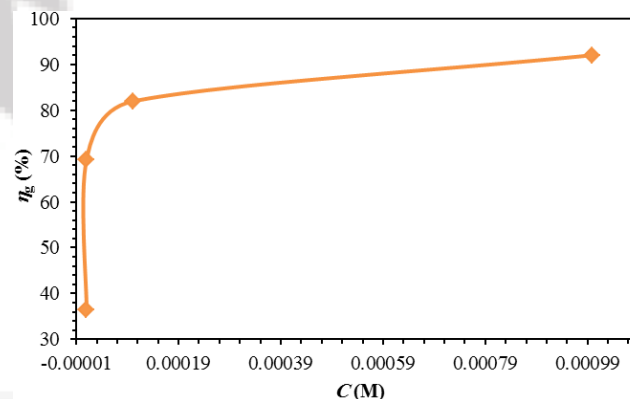


Figure 3: Relationship between the inhibition efficiency and inhibitor concentration for carbon steel at 298 K

Table 1: Gravimetric measurements parameters for carbon steel in 1 M HCl HCl containing various concentrations of TW80 at 298 K

TW80 conc. (M)	v (mg cm ⁻² h ⁻¹)	θ	η_g (%)
Blank	7.649	—	—
1 × 10 ⁻⁶	4.856	0.365	36.5
1 × 10 ⁻⁵	2.348	0.693	69.3
1 × 10 ⁻⁴	1.381	0.819	81.9
1 × 10 ⁻³	0.609	0.920	92.0

It is clear that the weight loss decreased (i.e. corrosion rate is suppressed) and the inhibition efficiency increased with increasing concentration of inhibitors. The maximum η_g values of 1×10⁻³ M of TW80 was found 92.0%. The inhibition of corrosion occurs due to the larger surface coverage (θ) of metal surface by inhibitor molecules [7].

3.2 Tafel polarization measurements

The effect of increased concentration of TW80 on the polarization curves of carbon steel in 1 M HCl, at 298 K is represented in Figure 4. The electrochemical parameters such as corrosion potential (E_{corr}), corrosion current density (i_{corr}), cathodic Tafel constant (β_c), anodic Tafel slope (β_a) and inhibition efficiency (η_p) are calculated and given in Table 2. The η_p was calculated from polarization measurements according to the relation given below [8];

$$\eta_p = \left(\frac{i - i^o}{i} \right) \times 100 \quad (3)$$

where i and i^o are uninhibited and inhibited corrosion current densities, respectively. It is clear that the i_{corr} decrease with increasing of the TW80 concentration; this indicates that inhibitor compounds are adsorbed on the metal surface and hence inhibition occurs.

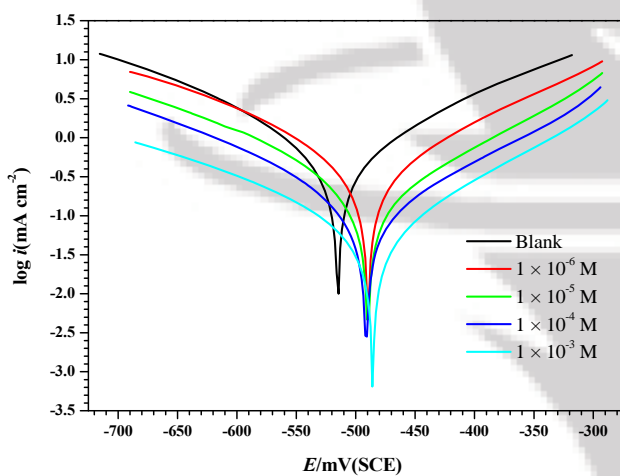


Figure 4: Polarization curves for carbon steel in 1 M HCl in the absence and presence of various concentrations of TW80

The polarization curves (Figure 4) show that TW80 has an effect on both, the cathodic and anodic slopes (β_c and β_a) and suppressed both cathodic and anodic processes. This indicates a modification of the mechanism of cathodic hydrogen evolution as well as anodic dissolution of iron, which suggest that inhibitor powerfully inhibits the corrosion process of carbon steel, and its ability as corrosion inhibitor is enhanced as its concentration is increased. The suppression of cathodic process can be due to the covering of the surface with monolayer due to the adsorbed inhibitor molecules.

Table 2: Polarization parameters for the corrosion of steel in 1 M HCl in the absence and presence of various concentrations of TW80 at 298 K

TW80 conc. (M)	$-E_{corr}$ (mV _{SCE})	i_{corr} (mA cm ⁻²)	β_a (mV dec ⁻¹)	$-\beta_c$ (mV dec ⁻¹)	η_p (%)
Blank	515.0	1.196	203	200	—
1×10^{-6}	489.7	0.698	187	195	41.7
1×10^{-5}	489.8	0.356	174	193	70.2
1×10^{-4}	491.2	0.203	175	181	83.0
1×10^{-3}	509.9	0.097	169	179	91.9

It can also be seen from Table 2 that the anodic and cathodic Tafel slope (β_a & β_c) decrease in the presence of TW80. This observation may be ascribed to changes in the charge transfer coefficient for the anodic dissolution and cathodic evolution of iron by virtue of the presence of an additional energy barrier due to the presence of adsorbed inhibitor. Further inspection of Table 2 also reveals that E_{corr} values do not show any significant change in the presence of various concentrations of the inhibitor suggesting that TW80 is mixed-type in 1 M HCl, which influences both metal dissolution and hydrogen evolution [9].

3.3. Electrochemical impedance spectroscopy (EIS)

Figure 5 shows the Nyquist plots for carbon steel in 1 M HCl in the absence and presence of TW80 at 298 K. The electrochemical parameters derived from Nyquist plots are calculated and listed in Table 3.

The values of charge transfer resistance (R_t) were given by subtracting the high frequency impedance from the low frequency one as follows [10]:

$$R_t = Z_{re}(\text{at low frequency}) - Z_{re}(\text{at high frequency}) \quad (4)$$

The values of electrochemical double layer capacitance (C_{dl}) were calculated at the frequency, f_{max} , at which the imaginary component of the impedance is maximal ($-Z_{max}$) by the following equation:

$$C_{dl} = (2\pi f_{max} R_t)^{-1} \quad (5)$$

The values of percentage inhibition efficiency (η_i) were calculated from the values of R_t according to the following equation [11]:

$$\eta_i = \left(\frac{R_t - R_t^o}{R_t} \right) \times 100 \quad (6)$$

where R_t and R_t^o are the values of the charge transfer resistance in the presence and absence of TW80, respectively.

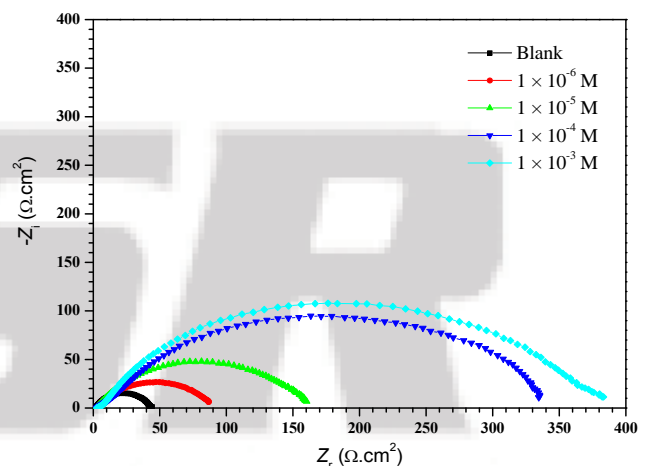


Figure 5: Nyquist plots for carbon steel in 1 M HCl in the absence and presence of various concentrations of TW80

The impedance data listed in Table 3 indicates that the values of both R_t and η_i are found to increase by increasing the TW80 concentration, while the values of C_{dl} are found to decrease. This behavior was the result of an increase in the

surface coverage by the inhibitor molecules, which led to an increase in the inhibition efficiency.

The decrease in C_{dl} values may be considered in terms of Helmholtz model [12]:

$$C_{dl} = \frac{\epsilon \epsilon_0}{d} \times S \quad (7)$$

where ϵ_0 is the permittivity of space ($8.854 \times 10^{-12} \text{ Fm}^{-1}$), ϵ is the local dielectric constant, d is the thickness of the film and S is the surface area of the electrode. In fact, the decrease in C_{dl} values can result from a decrease in local dielectric constant and/or an increase in the thickness of the electrical double layer [13]. The impedance spectra for the Nyquist plots were analyzed by fitting to the equivalent circuit model shown in Figure 6, which has been used previously to model the steel/acid interface. The circuit comprises a solution resistance R_s shorted by a constant phase element (CPE) that is placed in parallel to the charge transfer resistance R_t . The value of the charge transfer resistance is indicative of electron transfer across the interface. The use of the CPE, has been extensively described in the literature [14,15] and is employed in the model to compensate for the inhomogeneities in the electrode surface as depicted by the depressed nature of the Nyquist semicircle.

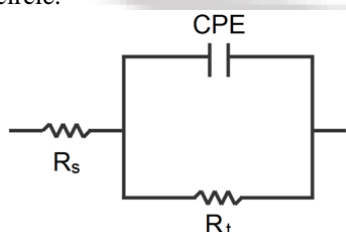


Figure 6: The equivalent circuit model used to fit the impedance data for carbon steel

The introduction of such a CPE is often used to interpret data for rough solid electrodes. The impedance, Z , of the CPE is:

$$Z_{CPE} = [Q(j\omega)^n]^{-1} \quad (8)$$

where the coefficient Q is a combination of properties related to different physical phenomena like surface inhomogeneous, electro-active species, inhibitor adsorption, porous layer formation, etc., j is an imaginary number ($j^2 = -1$), ω is the angular frequency ($\omega = 2\pi f$) and the exponent n has values between -1 and 1 . A value of -1 is a characteristic for an inductance, a value 1 corresponds to a resistor, and a value of 0.5 can be assigned to the diffusion phenomenon [16].

Table 3: Impedance parameters for the corrosion of steel in 1 M HCl in the absence and presence of various concentrations of TW80

TW80 conc. (M)	R_s (ohm.cm ²)	R_t (ohm.cm ²)	C_{dl} (μF cm ⁻²)	η_i (%)
Blank	2.3	37.4	311.5	—
1×10^{-6}	2.9	87.4	165.1	57.2
1×10^{-5}	2.6	160.6	105.4	76.7
1×10^{-4}	4.7	343.1	102.0	89.1
1×10^{-3}	3.7	377.1	88.8	90.1

3.4. Adsorption isotherm

The average values of θ ($\eta/100$) obtained from gravimetric, polarization and impedance measurements were tested graphically by fitting different adsorption isotherms, including the Freundlich, Temkin and Langmuir models. The correlation coefficient (R^2) was used to determine the isotherm that best fit the experimental data. A plot of C/θ versus C (Figure 6) gives a straight line with an average correlation coefficient of unity and a slope of nearly unity (0.9198) suggests that the adsorption of TW80 molecules obeys Langmuir adsorption isotherm. Langmuir adsorption isotherm expressed by the following equation [17]:

$$\frac{C}{\theta} = \frac{1}{K_{ads}} + C \quad (9)$$

where C is TW80 concentration and K_{ads} is the equilibrium constant for the adsorption-desorption process. The value K_{ads} calculated from the reciprocal of the intercept of isotherm line as $1.43 \times 10^8 \text{ M}^{-1}$. The high value of the adsorption equilibrium constant reflects the high adsorption ability of this inhibitor on the carbon steel surface. The standard free energy of adsorption of the inhibitor (ΔG_{ads}^o) on the carbon steel surface can be evaluated with the following equation;

$$\Delta G_{ads}^o = -RT \ln(55.5 K_{ads}) \quad (10)$$

According to equation (10) the value of ΔG_{ads}^o was calculated as $-57.4 \text{ kJ mol}^{-1}$. The negative value of standard free energy of adsorption indicates spontaneous adsorption of TW80 molecules on the carbon steel surface and also the strong interaction between inhibitor molecules and the metal surface [18].

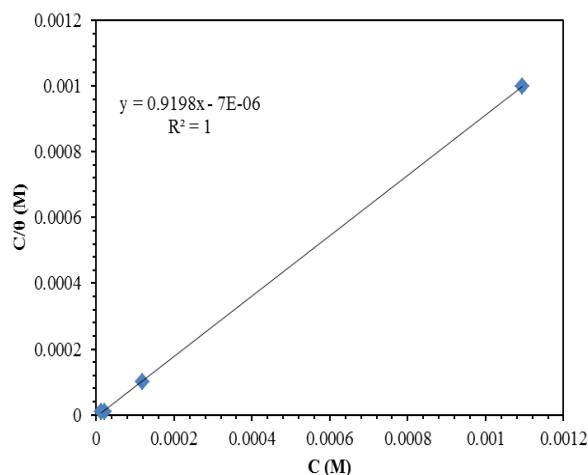


Figure 6: Langmuir adsorption plots of carbon steel in 1 M HCl solution containing various concentrations of TW80

Generally, absolute values of ΔG_{ads}^o up to 20 kJ mol^{-1} are consistent with physisorption associated with electrostatic adsorption, while those around 40 kJ mol^{-1} or higher are associated with chemisorption as a result of the sharing or transfer of electrons from organic molecules to the metal surface to form a coordinate type of metal bonds [19].

Here, the calculated ΔG_{ads}^o values are higher than 40 kJ mol⁻¹, indicating that the adsorption mechanism of TW80 on the carbon steel in 1 M HCl solution is chemical adsorption.

4. Conclusions

- 1) TW80 acts as a good inhibitor for the corrosion of carbon steel in 1 M HCl, and the inhibition efficiency increase with the inhibitor concentration, while decrease with the temperature.
- 2) The adsorption of the TW80 on the carbon steel surface obeys the Langmuir adsorption isotherm.
- 3) The potentiodynamic polarization curves indicated that TW80 behaves as a mixed-type inhibitor.
- 4) EIS results indicate that the C_{dl} decrease when these inhibitors are added; this due to adsorption of TW80 on the steel surface.

5. Acknowledgement

The authors are greatly thankful to the Egyptian Petroleum Research Institute (EPRI) fund and support.

References

- [1] M. Behpour, S. M. Ghoreishi, M. Khayatkashani, N. Soltani, Green approach to corrosion inhibition of mild steel in two acidic solutions by the extract of Punica granatum peel and main constituents, *Materials Chemistry and Physics* 131 (2012) 621–633.
- [2] Yuming Tang, Guodong Zhang, Yu Zuo, The inhibition effects of several inhibitors on rebar in acidified concrete pore solution, *Construction and Building Materials* 28 (2012) 327–332.
- [3] Serpil Safak, Berrin Duran, Aysel Yurt, Gülsen Türkoglu, Schiff bases as corrosion inhibitor for aluminium in HCl solution, *Corros. Sci.* 54 (2012) 251–259.
- [4] E. Sadeghi Meresht, T. Shahrabi Farahani, J. Neshati, 2-Butyne-1,4-diol as a novel corrosion inhibitor for API X65 steel pipeline in carbonate/bicarbonate solution, *Corros. Sci.* 54 (2012) 36–44.
- [5] Mohammed A. Amin, M. A. Ahmed, H. A. Arida, Fatma Kandemirli, Murat Saracoglu, Taner Arslan, Murat A. Basaran, Monitoring corrosion and corrosion control of iron in HCl by non-ionic surfactants of the TRITON-X series – Part III. Immersion time effects and theoretical studies, *Corros. Sci.* 53 (2011) 1895–1909.
- [6] M.A. Migahed, A.A. Farag, S.M. Elsaed, R. Kamal, M. Mostfa, H. Abd El-Bary, “Synthesis of a new family of Schiff base nonionic surfactants and evaluation of their corrosion inhibition effect on X-65 type tubing steel in deep oil wells formation water,” *Mater. Chem. Phys.* 125 (2011) 125–135.
- [7] T.P. Zhao, G.N. Mu, “The adsorption and corrosion inhibition of anion surfactants on aluminium surface in hydrochloric acid,” *Corros. Sci.* 41 (1999) 1937–1944.
- [8] Ahmed A. Farag, M.R. Noor El-Din, “The adsorption and corrosion inhibition of some nonionic surfactants

- on API X65 steel surface in hydrochloric acid,” *Corros. Sci.* 64 (2012) 174–183.
- [9] M.A. Quraishi, D. Jamal, “Dianils as new and effective corrosion inhibitors for mild steel in acidic solutions,” *Mater. Chem. Phys.* 78 (2003) 608–613.
 - [10] Ahmed M. Al-Sabagh, Notaila M. Nasser, Ahmed A. Farag, Mohamed A. Migahed, Abdelmonem M.F. Eissa, Tahany Mahmoud, “Structure effect of some amine derivatives on corrosion inhibition efficiency for carbon steel in acidic media using electrochemical and Quantum Theory Methods,” *Egyptian Journal of Petroleum* 22 (2013) 101–116.
 - [11] M.A. Migahed, A.A. Farag, S.M. Elsaed, R. Kamal, H.A. El-Bary, “Corrosion inhibition of steel pipelines in oil well formation water by a new family of nonionic surfactants,” *Chem. Eng. Commun.* 199 (2012) 1335–1356.
 - [12] Ahmed A. Farag, M.A. Hegazy, “Synergistic inhibition effect of potassium iodide and novel Schiff bases on X65 steel corrosion in 0.5 M H₂SO₄,” *Corros. Sci.* 74 (2013) 168–177.
 - [13] M. Kissi, M. Bouklah, B. Hammouti, M. Benkaddour, “Establishment of equivalent circuits from electrochemical impedance spectroscopy study of corrosion inhibition of steel by pyrazine in sulphuric acidic solution,” *Appl. Surf. Sci.* 252 (2006) 4190–4197.
 - [14] L. Larabi, Y. Harek, O. Benali, S. Ghalem, “Hydrazide derivatives as corrosion inhibitors for mild steel in 1 M HCl,” *Prog. Org. Coat.* 54 (2005) 256–262.
 - [15] Popova, E. Sokolova, S. Raicheva, M. Christov, “AC and DC study of the temperature effect on mild steel corrosion in acid media in the presence of benzimidazole derivatives,” *Corros. Sci.* 45 (2003) 33–58.
 - [16] Hulya Keles, Mustafa Keles, Ilyas Dehri, Osman Serindag, “The inhibitive effect of 6-amino-m-cresol and its Schiff base on the corrosion of mild steel in 0.5 M HCl medium,” *Mater. Chem. Phys.* 112 (2008) 173–179.
 - [17] W.H. Li, Q. He, S.T. Zhang, C.L. Pei, B.R. Hou, J. *Appl. Electrochem.* 38 (2008) 289–295.
 - [18] E. Cano, J.L. Polo, A. La Iglesia, J.M. Bastidas, *Adsorption* 10 (2004) 219–225.
 - [19] G. Quartarone, L. Ronchin, A. Vavasori, C. Tortato, L. Bonaldo, *Corros. Sci.* 64 (2012) 82–89.

Author Profile



Ahmed A. Farag received the B.Sc., Master and Ph.D. degrees in Chemistry from Science Faculty, Al-Azhar University/ Egypt in 2002, 2007 and 2011, respectively. I worked in National Research Center (NRC), Polymers and Pigments Department/Egypt until 2007. Now I am working in Egyptian Petroleum Research Institute (EPRI), Petroleum Applications Department/Egypt from 2007 until now.